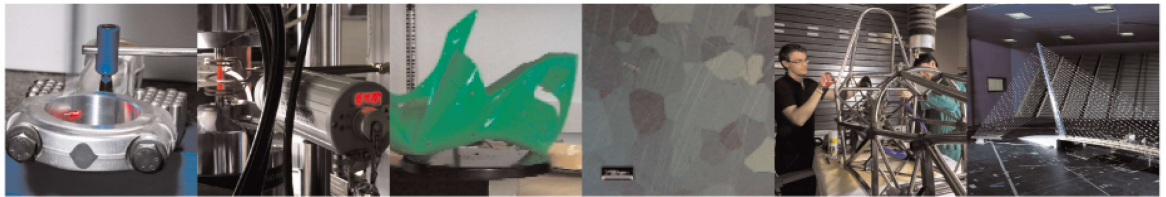




**POLITECNICO**  
MILANO 1863

DIPARTIMENTO DI MECCANICA



## Manufacturing and performance of 3D printed plastic tools for air bending applications

Zaragoza V.G.; Rane K.; Strano M.; Monno M.

This is a post-peer-review, pre-copyedit version of an article published in Journal of Manufacturing Processes. The final authenticated version is available online at:

<http://dx.doi.org/10.1016/j.jmapro.2021.04.045>

This content is provided under [CC BY-NC-ND 4.0](https://creativecommons.org/licenses/by-nc-nd/4.0/) license



# Manufacturing and performance of 3D printed plastic tools for air bending applications.

Veronica Geraldine Zaragoza<sup>a</sup>, Kedarnath Rane<sup>b</sup>, Matteo Strano<sup>b\*</sup>, Michele Monno<sup>b</sup>

<sup>a</sup>MUSP, Str. della Torre della Razza, Piacenza, 29122, Italy

<sup>b</sup>Politecnico di Milano, Dipartimento di Meccanica, Via G. La Masa, 1, 20156, Milan, Italy

\*corresponding author: [matteo.strano@polimi.it](mailto:matteo.strano@polimi.it)

---

## Abstract

In the sheet metal forming industry, rapid tools, especially those made of polymeric materials, are increasingly used for small to medium volume productions, to compress the times and costs of tooling. The present work is aimed at evaluating the performance of 3D printed tools for sheet metal V-die air bending process. Samples made of polycarbonate and polylactide were characterized through compression tests, using different printing strategies, to verify the effect of the printing parameters on the strength of the materials. FEA simulations of air bending were performed in order to predict the state of stress and strain of the plastic tools. Polymeric dies were then produced and used for repeated V-bending tests of metal sheets. The endurance and performance of the 3D printed tools were evaluated by analysing the changes in their surface and the repeatability of the bending angle after springback. The results show how the polymeric materials and their printing parameters influence the performance of the polymeric tools. Among the various tested configurations, the PLA dies, printed with a printing pattern of 45-90-45 degrees exhibit the best performance.

*Keywords:* Sheet metal bending; rapid tools; Additive manufacturing; 3d printing; Polymeric materials; resilience

## 1. Introduction

In the sheet metal forming industry, air bending is one of the most common manufacturing processes. Like other sheet metal forming processes, it changes the shape of a workpiece, through the plastic deformation of a metal sheet keeping a constant volume. Sheet metal air bending with V-shaped metal dies is widely used in industrial production because of its flexibility (different bend angles can be obtained with a single tool set with a given sheet material), its productivity (a single bend can be produced in a matter of seconds) and its acceptable repeatability of results. However, nowadays the automotive and aeronautical sectors are shifting their focus to a more customised production, thus facing an increasing demand for smaller batch productions, where the flexibility of air bending tools takes a higher importance [1]. Likewise, it has been shown that in times of crisis where having fast reaction times is essential, the ability to produce parts using short production cycles, e.g. by additive manufacturing technologies, becomes a key factor in increasing the resilience of the industrial system [2].

The conventional V-shaped die used in air bending is made of metal, generally tool steel, because its expected life should be long, and its bending performance is effective and long lasting. However, in a batch production or a customized part production, where sheet thickness and material may change very frequently, changing the die and the punch for each type of product might become not economical. For this reason, the concept of rapid tools emerged not less than 30 years ago [3]. Recently, the interest towards rapid and flexible tools is growing again, due to improved quality of additive manufacturing technologies and materials. The growing demand in the reduction of production times and costs increases the need for faster response times and more efficient means to produce prototypes and tools in the short term. As a result, the use of rapid tool technologies, such as 3D printing, using advanced polymeric materials and composite materials to manufacture sheet forming dies arises. A typical polymeric material used for flexible rapid tools for sheet metal forming is polyurethane, as shown by several authors which analysed its failure modes [4] and performance [5] in bending, its durability in deep drawing [6]. Polyurethanes (PU) have been frequently used for tooling, in its three forms: thermoset, thermoplastic and rubber. Rubber PU is the material of choice in rubber pad forming [7] and flexforming [8] processes. Polyurethane tools can be produced in many different ways: thermoset PU can be rapidly machined to the desired dimensions and tolerances [9]; thermoset PU can also be poured by casting and, if required, it can be coated with a hard coating, e.g. by electrical arc spraying [10]. Hard coatings are useful to increase the wear resistance of rapid tools. A more flexible and cost-efficient option is to produce the rapid tools by means of additive manufacturing processes, such as Selective Laser Melting [11], which can be used for metal tools, or Fused Deposited Modelling, which can be used for thermoplastic polymeric tools.

Fused Deposited Modelling (FDM) is one of the most common techniques used for 3D printers and has become one of the most popular rapid prototyping (RP) techniques in the last decade [12]. A more general and comprehensive definition of the technology is Extrusion based Additive Manufacturing (EAM). Nakamura et al. [13] analysed the efficiency of the V-bending process for aluminium and steel sheets using different combinations of tools made of PLA and steel; the study showed that plastic tools can be used to bend metal sheets, being noticed that to improve the dimensional accuracy of the products it is effective to use a combination with a steel punch and a plastic die. However, the strength of parts manufactured by EAM is lower than the strength obtained with other manufacturing techniques (for example, injection moulding). This may have an effect in the bend angles obtained, with respect to steel tools. For this reason, it is desirable to develop an approach to reduce the elastic deformation of plastic tools made by EAM.

In the literature, some approaches can be found with respect to improving the strength of 3D printing components. Some authors have studied the influence of printing parameters (layer thickness, orientation, raster angle, raster width and air gap) on the mechanical properties of the tool (tensile, flexure and impact strengths). Among these parameters, it has been found that the build orientation, the raster parameters and the air gap are the ones that can influence more the mechanical properties of the part [14]. Using ABS samples, Hernandez et al. [15] evaluated the effect of 5 different printing orientations in a plane XYZ, finding that the samples printed at 0° in the XY plane offer a strongest resistance in compression and flexure, having the greatest modulus of elasticity; while the samples printed at 90° in the XY plane shows a strongest behavior in tension, having the largest tensile strength and lowest modulus of elasticity. For its part, Sood et al. [16] found that the reduction in distortion is a necessary requirement for good strength. Then, the use of a small number of layers, and a proper raster orientation can help to increase the performance of the tool. The authors have shown that the increase of raster angle in the samples allow to produce smaller rasters, which are subjected to less distortion, helping to improve the strength. The raster angle used by default in EAM is 45°- 45°. However, there is an important interaction between the build mechanism in EAM which does not allow to establish a single independent parameter as the best condition to obtain higher performances. Other methods to improve the strength of EAM printing materials, independent of the printing parameters, also include the use of filler materials such as carbon fibres or composites resins as an addition to the printing process. The layers and the direction of the fibres introduce an anisotropic effect that greatly influences the overall strength of the 3D printed part. Belter et al. [17], for example, showed a technique to increase the strength in the manufacture of thermoplastic parts by EAM, carefully placing holes in the printed parts and fill them with high-strength resins. This system is limited by the strength of the thermoplastic and offer only slight improvements over standard EAM printing methods.

The approach presented in this article involves the design and production of V-air bending polymeric dies using different printing strategies, with the aim of evaluating the performance of this type of tools in the sheet metal bending process. The printing filaments considered for this study were PLA and PC. These two materials are chosen because they belong to the category of thermoplastics with good values of mechanical strength (tensile strength around 60 MPa) that can be printed using EAM technology. Besides, PLA and PC have very good printability with conventional EAM machines and they are among the most inexpensive EAM materials [18].

The printing parameters such as raster width, raster angle, nozzle tip diameter and printing orientation were analysed with the different materials, in order to evaluate the optimal printing conditions to obtain higher mechanical strength of the tools. During the study, special attention was paid regarding the effect of raster angle on the strength of the tools, as suggested by Sood et al. [16]. A total of 5 different combinations of angles were used for the printing pattern, during the 3D printing of the pieces. To the authors' knowledge, no published work has been found that investigates in detail the effect of this parameter during the performance of the tools in sheet metal bending.



## 2. Case study on polycarbonate V-dies

The goal of the first case study, used as the starting point of this research, was to assess if a 3D printed polymeric insert, made of polycarbonate (PC), was able to produce a repeatable bending angle  $\alpha_f$ , with no relevant or evident geometrical damage on its surface. The PC die had to sustain a small batch of V-die air bending tests with sheet metals.

The polymeric die was produced using the FDM (Fused Deposition Modeling) technology with a Stratasys Fortus 380 machine. During the sheet bending tests, the polymeric die insert is subject mainly to compression stresses. Therefore, before starting the bending tests, to select the optimum 3D printing process parameters, a material characterization campaign was performed through a series of compression tests. Cylindrical compression samples were 3D printed in polycarbonate, using different printing strategies, as show in Table 1. The parameters to be evaluated are the raster width (w), the nozzle tip diameter (d), the layer thickness (s) and the printing orientation.

The print orientation is the build orientation followed while printing the sample, instead the printing pattern regards mostly the raster angle used during the printing process. For the compression tests, changes in mechanical properties were measured considering two different construction configurations (vertical and horizontal). However, the printing pattern selected in the case of polycarbonate corresponds to the typical value used by FDM, with a raster angle of 45°-45°. Regarding the other selected parameters, it is important to highlight that there is a correlation between the diameter of the tip of the nozzle (d) and the layer thickness (s). In the printer, when selecting the value for the first condition (for example, the type of tip), the machine automatically suggests a standard value for the second value. Thus, the thickness of the layer is fixed during the printing process, considering only variations in the nozzle tip diameter.

Table 1. Printing parameters polycarbonate samples

Polycarbonate	
Tip diameter d (mm)	T12 (d= 0.305 mm) - layer thickness 0.178mm
Layer thickness s (mm)	T16 (d= 0.406 mm) - layer thickness 0.254mm
Raster width w (mm)	0,4 mm 0,6 mm
Printing orientation	  Vertical Horizontal
Printing pattern	45°-45°

The compression tests were performed following the standard for compressive properties of rigid plastics (*ASTM D695*)[19], using a ram velocity equal to 2 mm/min. Measurements on the Young's modulus  $E$  (GPa) and the yield strength  $Y_s$  (MPa) were considered for comparing the printing parameters; the obtained results are shown in the Figures 1.a and 1.b.

These figures allow to determine the process parameters that offer better expected mechanical properties (among the tested ones). The confidence intervals for both variables are rather large and there is no combination of parameters that clearly dominate the others. Nevertheless, the highest mean  $E$ -value and  $Y_s$ -value has been mostly obtained by printing with the T16 nozzle. For the  $E$ -values using a raster width  $w=0.6$ mm, the measurements seem to have lower variability. The horizontal orientation seems to be preferable in terms of yield stress. The raster width does not have a clear effect on  $Y_s$ . Overall, the compression characterization tests allow to predict that a good performance of the polymeric die inserts can be obtained by printing the sample with a horizontal orientation, a tip diameter T16 and a raster width of  $w=0.6$  mm.

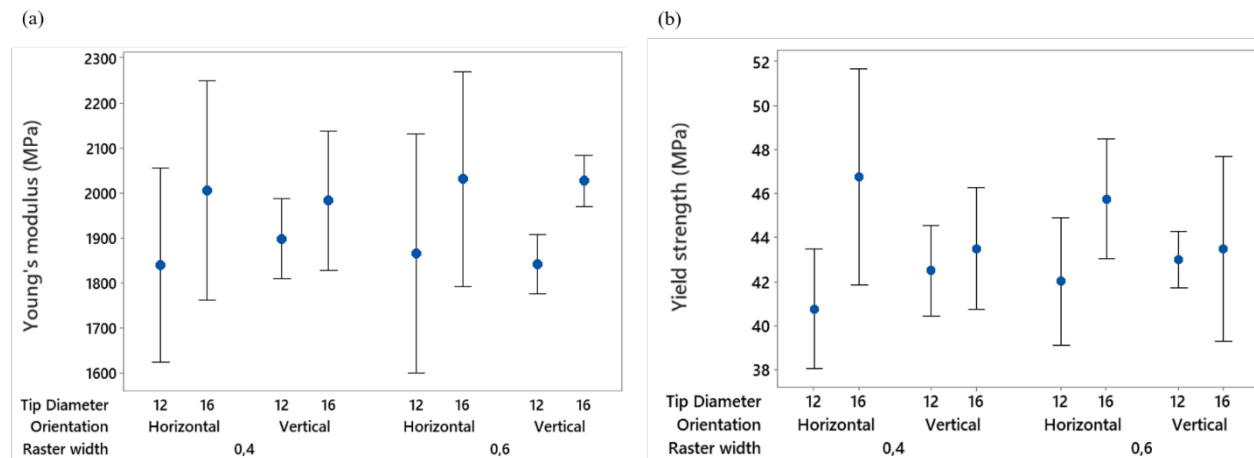


Figure 1. (a) Interval plot of Young's modulus for polycarbonate, (b) interval plot of yield strength for polycarbonate

To understand better if the printing parameters can have an effect in the mechanical properties of the final part, it is interesting to compare the values obtained from the compression tests with the theoretical values, expected from the data sheet of the material (Stratasys Fortus 3D printer datasheet). The 3D printed polycarbonate using the Stratasys printer has a compressive nominal Young's modulus  $E=1.57$  GPa and yield strength  $Y_s=64$  MPa; however, the experimental test shows that with the parameters used, it is possible to obtain more rigid polycarbonate samples but with lower mechanical strength. The best experimental mean values obtained for the printed polycarbonate are around 2.1 GPa and 46 MPa, for the  $E$  and  $Y_s$ , respectively.

## 2.1 FEM simulation of the bending operations

The mechanical characterisation of the 3D printed PC presented above has been used as an input for running FEM simulations. Before printing the V bending dies for the experimental tests, numerical simulations were performed to estimate the magnitude of stresses and strains in the tools. Considering a sheet metal made of a low strength steel and using the die geometry in Figure 2, a set of Finite Elements Models (FEM) was run for bending at  $\alpha_f = 90^\circ$ , with a changing thickness from  $t_0 = 0.5$  mm to  $t_0 = 2$  mm.

A two-dimensional "base" model was constructed using the commercial package ABAQUS/CAE as shown in Fig. 2. For the analysis, the punch and the metal support for the insert were modelled as rigid materials, while the polymeric die and the metallic sheet were modelled as deformable parts. Since the only interest is the concentration of stresses of the die during this bending, the metallic support and the punch in the software are considered as "wire" structure while the die and the sheet are modelled with 2D plain strain "brick" elements. The mesh of the tools has been generated with a total of 713 linear quadrilateral elements of type CPS4R, with a finer mesh in the areas where a higher accuracy is required. These kinds of elements have been chosen because they allow to achieve precision in the results without increasing too much the computational cost. The mechanical properties of the low strength steel were selected considering the typical values for this type of materials, with a Young modulus of  $E = 200$  GPa and a yield strength  $Y_s = 300$  MPa, while the properties of the PC were taken from the compression test results. A "surface to surface" contact type with finite sliding formulation and a friction coefficient of 0.3 has been created. Following a dynamic analysis with Abaqus explicit, the process is set to perform the bending process with a punch stroke adapted according to the sheet thickness to be bend.

Once the surfaces and the interaction between them are assigned, the boundary conditions to simulate the behaviour of the components during the experimental test must be defined. For the numerical model, the force used to bend the sheet until a certain angle is not defined through a load but through the velocity to move the punch along a path. The movement of the punch is settled to be just in vertical direction, without other rotational or translational degree of freedom. Furthermore, the metallic base that is used as a support for the insert must be fixed at the bottom, so its movement must be restrained in all directions.

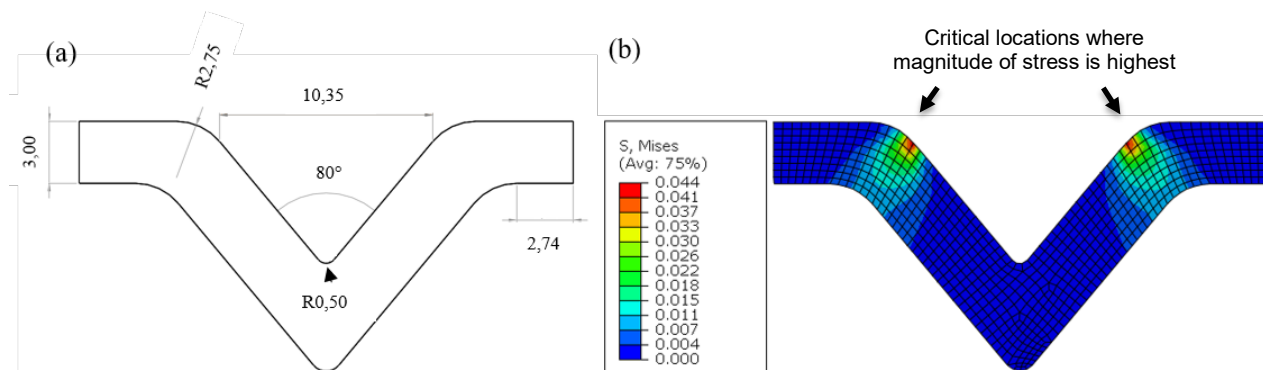


Figure 2. (a) Die geometry of polycarbonate insert (all units in mm), (b) Von Mises stress concentration on the surface (MPa) at the end of the punch stroke. FEM analysis on the V-shape polycarbonate die using a carbon steel sheet with  $t_0=1.5$ mm.

Table 2. Von Mises stress  $\sigma^*$  and equivalent strain concentration on polycarbonate die with different sheet thickness.

Sheet thickness $t_0$ (mm)	Von Mises stress $\sigma^*$ (MPa)	Load ratio $\sigma^*/Y_s*100$	Equivalent Strain (%)
0.5	5	11%	3
1	19	41%	10
1.5	44	96%	21
2	70	152%	35

It can be observed that the stress concentration during bending operations is in the radius of curvature of the die. This must be considered the critical region for the stability of the tool geometry: any geometrical modifications of the dies during bending are expected to occur in this area. The maximum values of Von Mises stress  $\sigma^*$  and equivalent strain for each sheet thickness considered in the analysis are presented in Table 2. Clearly, the larger stress and strain values on the die have been observed when bending with  $t_0 = 2$  mm, which is the thicker sheet simulated. As established during the compression analysis of cylindrical PC samples, the maximum yield strength of the printed polycarbonate is around 46 MPa. Then based on the FEM analysis it can be highlighted that with the PC dies, it is expected to bend mild steel sheets up to a thickness of 1.5 mm without a risk of permanent changes in the surface, with  $\sigma^* = 44$  MPa, which is close to the maximum  $Y_s$  value. After that threshold, using a higher thickness of 2 mm, the corner radii of the die might start to suffer permanent deformations even after the first bend, because the stress concentration in the critical area reaches values as large as of 70 MPa, way above the PC yield strength.

## 2.2 Stability of the bending process using polycarbonate dies

For the bending analysis, a V-shaped polycarbonate insert (cross sectional geometry as in Fig. 2, length of 10.35 mm) was printed and used for the bending of two types of steel (a low strength carbon steel C45 and a stainless steel AISI 430), both with a thickness  $t_0 = 1.5$  mm, which is supposed to be the maximum valued that can be sustained by the PC tools. The experiments were carried out using a metallic V-shaped punch with an opening angle of  $88^\circ$  and a metallic support where a polymeric insert with an opening angle of  $80^\circ$  was fixed. The tools were mounted onto a hydraulic press EASYPRESS which has a maximum bending force of 6.5 tons. The punch stroke was set to get a target angle after springback  $\alpha_f = 90 \pm 0.5^\circ$ . A total sequence of 100 bending tests, using 50 sheets of C45 and 50 sheets of AISI 430, was performed to study the stability of the polymeric tools. To adjust the stroke of the punch to reach the target angle, 20 preliminary bend cycles for each material were done; as consequences, a total of 70 bending were produced with each type of sheet. A tonnage of approximately 12 kN/m has been applied for the low strength steel and of about 20 kN/m for the stainless steel. The sheet samples are rectangular with dimensions 105x95mm. To ensure the repeatability of the measurement, the samples have all been placed with their rolling direction perpendicular to the die length and the bending is always done exactly in the mid-point of the sheets.

To evaluate the efficiency of the use of polycarbonate tools as flexible inserts during the bending process, it is necessary to verify the capability of the insert to obtain the target bending angle and analyse the changes occurred in the surface of the polymeric die during the bending process. To determine the stability of the part geometry, an analysis of the angle  $\alpha_f$  after springback is done.

The measurements were taken considering batches composed of 10 metallic sheets. The 50 effective bends using the C45 sheets were taken starting from the 20th to 70th fold (horizontal axis, figure 3), because the first 2 batches of 10 sheets were considered for the punch stroke calibration. Same situation with the AISI 430, where the target angle was measured between the 90th and 140th fold. The results in the figure 3 show that the mean values of the bending angle for both low strength carbon steel and stainless steel lay above  $90^\circ$  with values of  $91^\circ$  and  $90.25^\circ$ , respectively.

It can be noted that for the low strength carbon steel, the high increase in the angle value occurs mainly during the bending of the first batch after punch stroke calibration. From the 30<sup>th</sup> fold, the overall behaviour of the die seems to stabilize, i.e. the average obtained angle does not significantly increase any more. Despite the die has been 3D printed with a 100% theoretical infill density, some residual porosity between roads and between layers is still present, inherent to the FDM process. During the bending cycle, and after the 30<sup>th</sup> bending, it is possible that the compression stress given to the die by the punch, through the sheet metal, can help close any residual porosity and the mechanical response of the die stabilises.

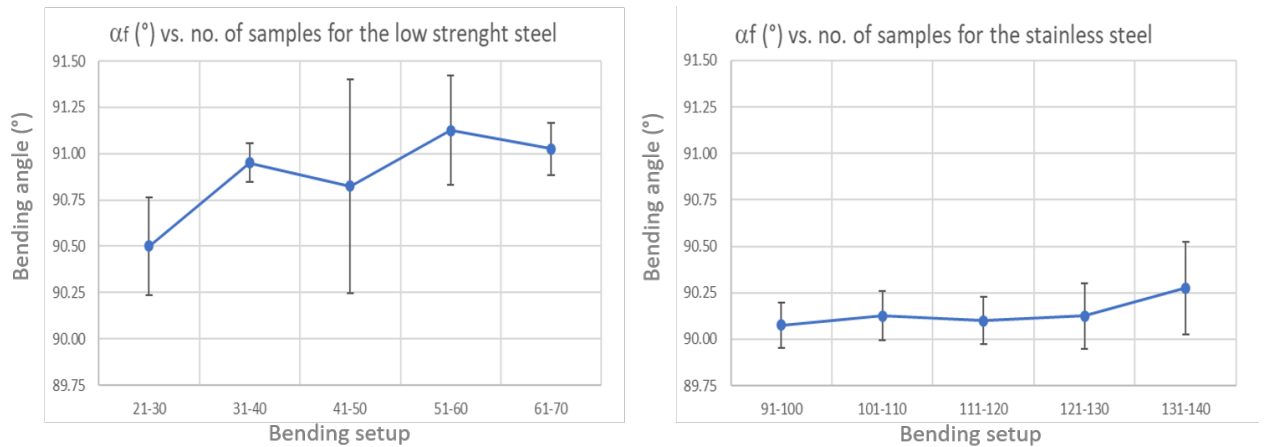


Figure 3. Interval plots for the bending test with a polycarbonate die.

A further confirmation of the die stabilization can be observed during the bending test with stainless steel, where the angle remains almost constant, despite the increase in tonnage compared to the first 70 bends. An increase in the final bent angle and an increase in the dispersion of data around the mean can be observed after the 130th cycle. The stainless-steel sheets, despite being teste after the mild steel, exhibit a smaller standard deviation of the results, because of a better formability and inherent quality of the stainless steel.

Although the numerically calculated stress at the die corners should be below the yield stress, according to the FEM simulations, after several tests the die might as well undergo permanent deformation, due to low cycle fatigue. Therefore, it is possible to assume that after a sequence of bending cycles, the 3D printed plastic die insert tends to open its width and broaden its corner radii as the loading/unloading cycles continue during the test. Using a profilometer it is possible to check the changes in the die profile on the most critical areas. The measurements are made at the end of the whole sequence of bending tests. The measurements are taken using 3 different positions along the length of the die. A comparison was made between the experimental values of the radius of curvature obtained after bending and the values designed in the CAD model. After the bending of all sheets, it was noticed an increase in the values of the radius of curvature of the polycarbonate die corners. The variation of the die edges at the end of the bending tests is around 45% with respect to the designed values.

The air bending of metal sheets using polycarbonate dies is feasible for very small batches, however, the resistance of polycarbonate dies printed by EAM is not enough to avoid permanent deformation of its edges during the bending process of steel sheets 1.5 mm thick or thicker.

### 3. V-air bending process with PLA tools

The brief study presented in Section 2 has shown the mechanical resistance of 3D printed polycarbonate dies in sheet metal bending process. However, seeking to improve the performance of rapid polymeric tools, a deeper study has been carried out considering a material with higher performance and a different printing strategy. PLA is a very common and inexpensive 3D printing feedstock, but it has a higher compression strength than PC. Due to its better printability, it can be 3D printed even with a low cost, “consumer” type FDM printer. In a very recently published paper [20], it has been demonstrated that 3D printed PLA tools are sufficiently stable for sheet metal forming and provide similarly good results as metallic tools in terms of formability.

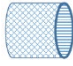





The aim of this second study case is to evaluate whether changes in the printing strategy can improve the mechanical properties of the part, allowing to obtain more stable tools that are subject to less deformation during the bending process. A new polymeric die made of polylactide (PLA) was printed with a consumer 3d printer (Crealitty Ender 3).

The printing strategy used on this study to measure the mechanical strength under compression, considers only changes in the printing pattern used. While the standard pattern used on 3D printing (as established above) is 45°-45°, it is possible to modify the G-codes generated during printing to create patterns with different angles combinations ranging from 0° to 90°. Changes in the raster angle during the printing process could help reduce the effect of anisotropy, common in EAM samples, which could influence the overall mechanical strength of the part.



The tested experimental conditions are shown in Table 3. The orientation, raster width, layer thickness and tip diameter have been selected as the best conditions for quality, according to section 2 and to the data sheet of the provider of the filament.

Table 3. Printing parameters PLA samples

PLA	
Tip diameter d (mm)	d= 0.40 mm
Layer thickness s (mm)	0.254mm
Raster width w (mm)	0.6
Printing orientation	 Horizontal
Printing pattern	45°-45° 
	0°-90° 
	45°-0°-45°-90° 
	45°-0°-45° 
	45°-90°-45° 

The results are shown in Figure 4, where the mean measured values and their 95% confidence intervals are shown for the elastic modulus  $E$ , the yield strength  $Y_s$  and the measured relative density  $\rho\%$ . The results indicate no statistically significant difference in the mean values of  $E$  and  $Y_s$ . As for the relative density, the 0°-90° clearly produces a lower value of  $\rho\%$  (95.8%), with respect to all other printing patterns (97.4%).

Slight difference in density can be related to presence of inter-bead porosity inside the samples due to the different infill orientation used to build the part. Usually, FDM parts of PLA are characterized to have some porosity in their structure[21]. From the results on the figure 4.c, a lower density value while printing with the orientation 0°-90° can be related to higher percentage of porosity in the samples. Likewise, the porosity effect may be also present when considering the long amplitude of the confidence interval obtained while printing with the orientations of 45°-0°-45° and 45°-90°-45°. The inter-bead porosity can have some consequences on the mechanical performance of the 3D printed parts, as established for Anderson and Al-Mahatma[21][22].

As seen in the Fig. 4, the confidence intervals obtained using a standard printing pattern of 45°-45° or a pattern combination of 45°-0°-45°-90° (surrounded for a red rectangle) are the smaller within the different tested combinations. Then, it is possible to establish these conditions as the ones who offer the most repeatable mechanical properties. On the contrary, the variability in the results of  $E$  and  $Y_s$  obtained with the 0°-90° and the 45°-0°-45° patterns are significantly worse (large amplitude), which means the repeatability on this samples is low. The researchers believe that one major cause of mechanical variability is the low accuracy of the printer, which can lead to greater variability in inter-bead porosity, especially when considering certain printing pattern combination. Inter-bead porosity has been correlated to reduced mechanical properties and reliability, higher mechanical properties have been reported in samples with low or no presence of inter-bead porosity[23].

As with polycarbonate samples, to better understand the effect of the printing parameters on the mechanical properties, the experimental values can be compared with the expected nominal values for the neat material. The used PLA is by Sharebot and the company does not provide the yield strength, neither in tension nor in compression. According to the CES Edupack database, the nominal values of a generic PLA in compression are around  $E = 3.3$  GPa and  $Y_s = 66$  MPa. The experimental mean values obtained from the tests are equal to or higher than the CES nominal values, with a mean  $E = 3.2$  GPa and  $Y_s = 69.5$  MPa, which means that regardless of the printing pattern, with the 3D printing technology, it is possible to obtain characteristics similar to those expected with the neat PLA.



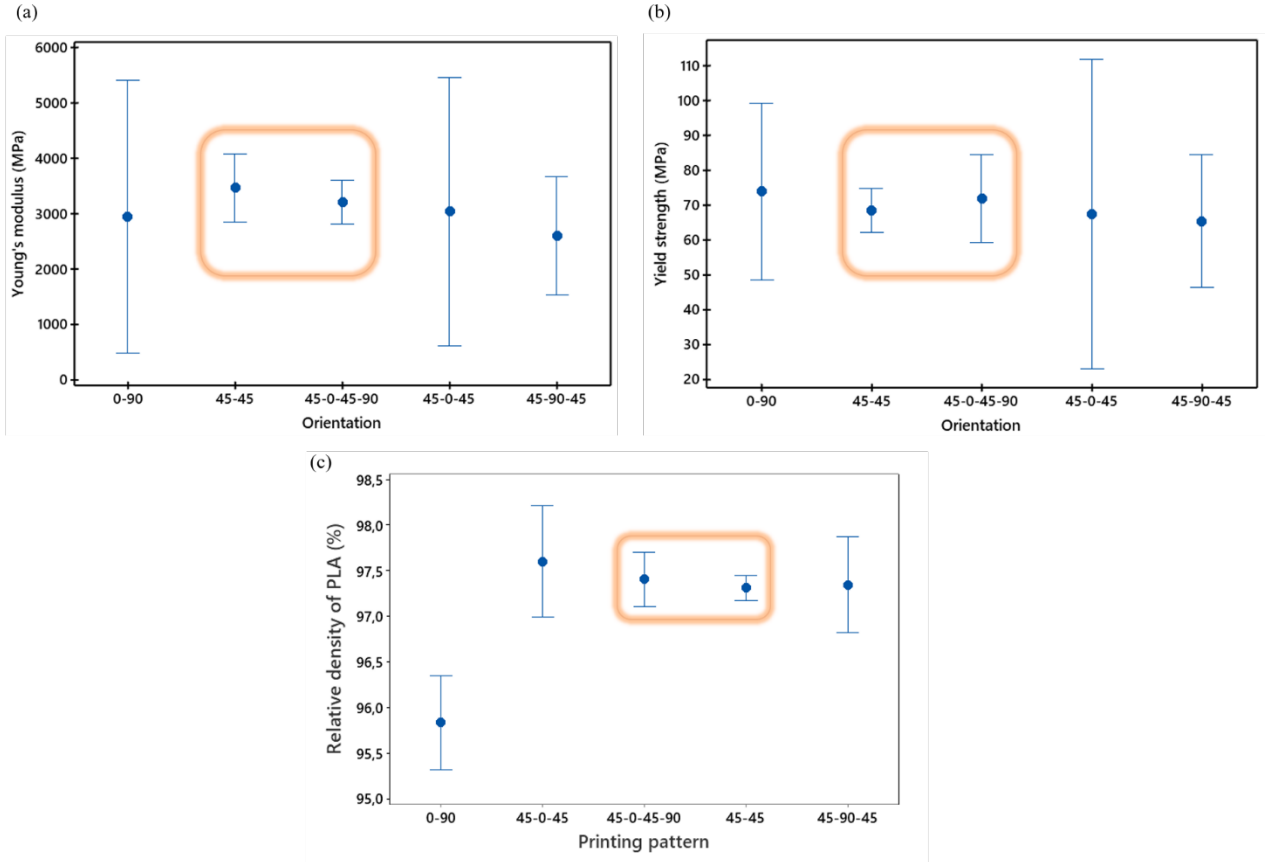


Figure 4. (a) Interval plots of Young's modulus for PLA, (b) interval plot of yield strength for PLA (c) interval plot of relative density, under the assumption of a full density for PLA of  $1.25 \text{ g/cm}^3$

Table 4 shows a comparison of the mechanical properties for both printed materials studied in compression. It can be noted that, regardless of the printing pattern used, the properties obtained with the printed PLA samples are better than those of the 3D printed polycarbonate: higher density, higher Poisson coefficient (i.e. lower compressibility), higher elastic modulus, higher yield stress.

Table 4. Comparison of average material properties for the printed cylinder samples.

Material	Density ( $\text{g/cm}^3$ )	Poisson's coefficient	Young's Modulus (MPa)	Yield Stress (MPa)
PLA	1.21	0.4	$3.20 \cdot 10^3$	69.50
Polycarbonate	<1.20	0.37	$1.94 \cdot 10^3$	43.47

### 3.1 Experimental setup – bending of PLA

A total of 5 die inserts of PLA are printed with EAM technology and using each of the printing pattern combinations studied during the compression test. The cross-sectional geometry of the V-shaped dies used for the analysis is shown in Figure 5.a. With respect to the die in Figure 2, the new die has a smaller width  $w$ , hence it allows bending to the same bend angle with a shorter punch stroke, but it is more stressed. Before starting the experimental tests, a new set of numerical simulations were performed to verify the new conditions of stress and strain in the tools. The sheet thicknesses tested in this case range from  $t_0 = 0.4 \text{ mm}$  to  $t_0 = 1.2 \text{ mm}$ . A two-dimensional “base” model with the new geometry was constructed using same procedure described at section 2.1.

After the analysis, it can be observed that the critical region for the highest stress concentration is still located at the die corners, as highlighted in Figure 5.b. The maximum value of Von Mises stress obtained for each sheet thickness is shown in table 5. As seen above, the maximum elastic limit of the printed PLA is around 70 MPa. According to the FEM analysis, the thickness of the steel sheet to bend during the experimental tests should be not thicker than 1 mm ( $Y_s = 59$  MPa), in order to avoid the plastic deformation of the die. Using a thicker sheet  $t_0 = 1.2$  mm, the stress value overcome the yield strength value of the material. Although the PLA is stronger than the PC, the limit on the maximum thickness predicted by the FEM is lower, because of the smaller die used in this case.

Table 5. Von Mises stress on PLA die with different sheet thickness.

Sheet thickness $t_0$ (mm)	Von Mises stress $\sigma^*$ (MPa)	Load ratio $\sigma^*/Y_s*100$
0.4	13	19%
0.6	29	42%
1	50	72%
1.2	73	105%

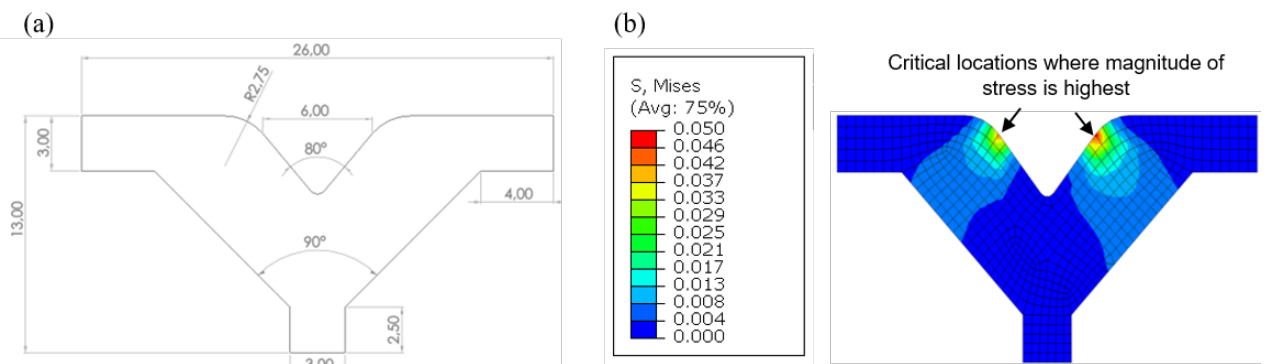


Figure 5. (a) Die geometry of PLA insert (all units in mm), (b) FEM analysis on the V-shape PLA die using a carbon steel sheet with  $t_0=1$ mm. Von Mises stress concentration on the surface at the end of the punch stroke (MPa).

The printed PLA dies as shown in Figure 6 were used for the bending aluminium and low strength carbon steel sheets, both with a thickness  $t_0 = 1$  mm. The experiments were carried out using the setup shown in Figure 6 (c). The press brake used for the experiments is a manual press SAR 1000. In this press, a V-shaped metal punch with an opening angle of  $88^\circ$ , two metal blocks and the V-shaped polymer inserts are mounted. The two metallic blocks attached to the punch were built as “stoppers” for the test, therefore, a constant target angle of  $\alpha_f = 90^\circ$  is not established, but still the tests are run with a constant punch stroke, for both types of materials. The stroke of the punch was calculated experimentally, considering a preliminary bending test with a set of 60 sheets (40 of aluminium alloy and 20 of steel). During this test, the sheets were bent to their maximum limit, where there is no possible further movement of the punch. At that point, the distance from the punch to the base is measured and the value obtained is used as the height for the design of the metal blocks that guide the stroke of the punch.

After the preliminary test, a new set of 60 sheets were used to evaluate the stability of the polymeric tools as shown in Figure 6 (d). The actual bending tests followed the same sequence as the preliminary tests, starting with the bending of 20 aluminium sheets, followed by a set of 20 steel sheets and ending with a new set of 20 aluminium sheets.

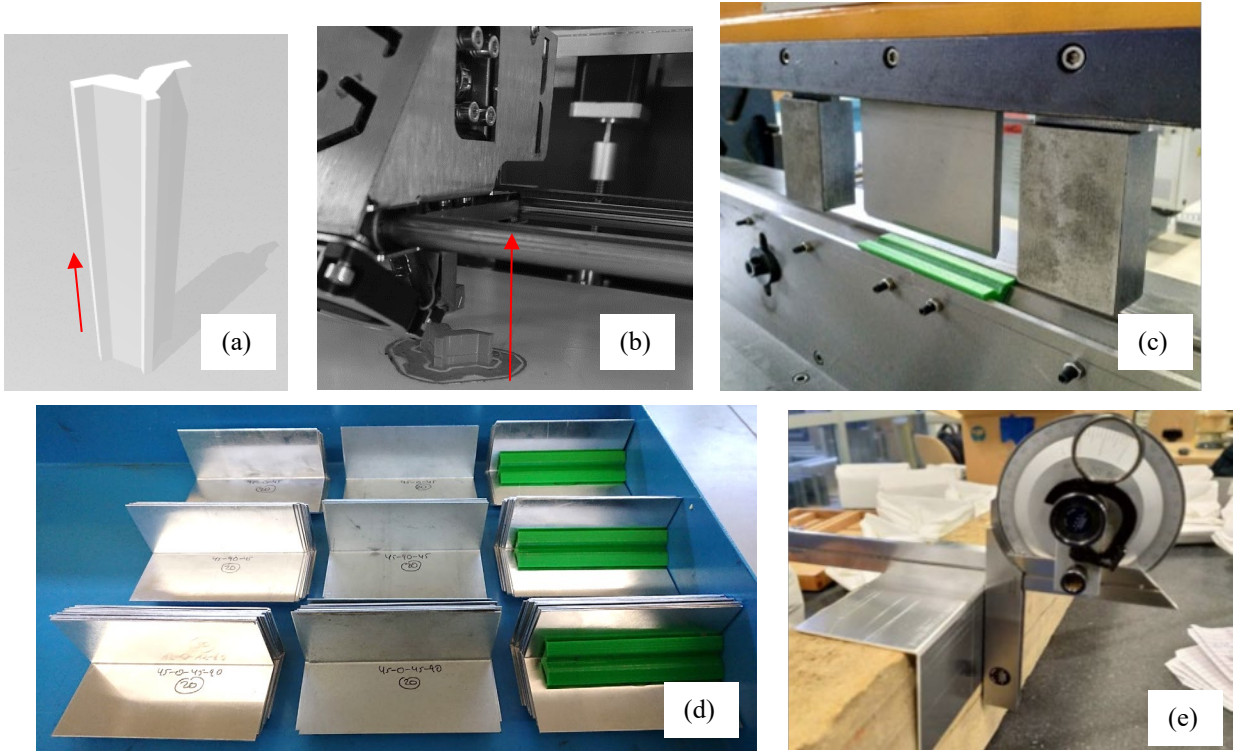


Figure 6. Experimental sequence realised for this sheet metal bending study: (a) 3D modelling of tool and slicing, arrow indicates building orientation for tools (b) 3D printing of dies with different printing configuration, (c) experimental setup for the bending test with polymeric dies (d) collection of sheets and dies after bending test (e) characterisation of sheet samples including bend angle measurements.

### 3.2. Stability of the bending process

To determine the stability of the bending process, an analysis considering the bend angle of the metal sheets has been performed as presented in Figure 6 (e). Since the experimental campaign comprises a different set of sheets and two materials to evaluate, the comparison is made considering the difference in the angle of each sheet bent with respect to the angle of the first sheet bent for each set. The calculation is shown in equation 1, where  $\alpha_1$  stands for the initial bend angle of each set and  $\alpha_i$  stands for the bend angle measured successively. In this way, it is possible to make the comparison between dies, focusing on the angle deviation respect to the first measurement and not in the individual values. The results obtained during the bending of 60 sheets are shown in Figure 7.

$$\alpha_i - \alpha_1 \quad (1)$$

From the figure 7, it is possible to observe that the dies printed with a printing pattern of  $45^\circ-45^\circ$ ,  $45^\circ-90^\circ-45^\circ$  and  $45^\circ-0^\circ-45^\circ-90^\circ$  show a stabilization in the angle deviation during the performance of the bending process (the confidence interval decreases). Surprisingly, the most stable behaviour is not observed with the standard  $45^\circ-45^\circ$  pattern, but with the alternated  $45^\circ-90^\circ-45^\circ$  pattern, for which the angle deviation never exceeds  $\pm 0.5^\circ$ . For these 3 mentioned printing patterns, the confidence interval of the second set of tests with the aluminium sheet is consistently lower than the one obtained with the first set. This is likely due to a compaction of the 3D printed layers. The bending stresses reduce the inter-bead porosity within the insert and its performance improves over the first 20+20+20 tests, therefore, as the bending of the sheets continues, the stiffness of the plastic tools increases slightly, increasing the dimensional accuracy of the bent sheet[24]. The presence of small air gaps or porosity between 3D printed roads was confirmed in this study by the relative density measurements, which are all between 96% and 98%.

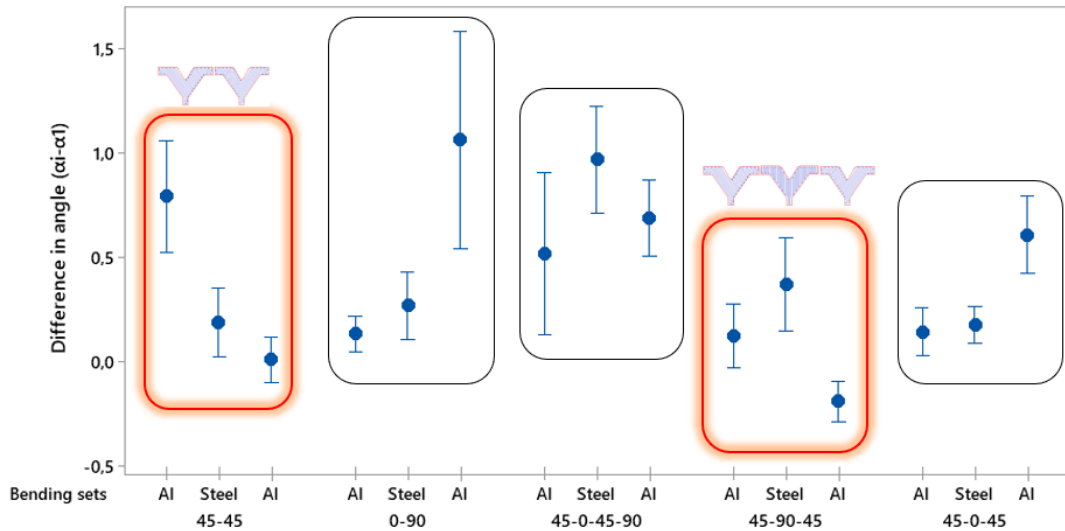


Figure 7. Interval plot for the bending test with different sets of metallic materials; each die has been tested with 60 bending cycles, in a sequence of 20 tests with aluminium, 20 with steel and then 20 again with aluminium.

On the other hand, die inserts with a printing pattern equal to  $0^{\circ}$ - $90^{\circ}$  and  $45^{\circ}$ - $0^{\circ}$ - $45^{\circ}$  have a more unstable performance over time, as can be seen by the increase of the difference in angle after bending few sheets. These two patterns showed the lowest repeatability during compression tests (fig 4), due to the high variability in the inter-bead porosity. If the porosity in the samples printed with these patterns is not uniform, it may be more difficult to achieve a compaction during the bending process that can help improve the mechanical performance of the part when subjected to high values of stress.

### 3.3. Surface analysis: geometrical profile and roughness

To have another source of information about the stability of the polymeric dies, an analysis of their surface geometry has been performed before and after the bending test. Using a profilometer, it is possible to verify possible changes in the die profile in areas of high stress concentration. Besides, their surface wear can be somehow correlated to a change of their surface roughness.

Regarding the die profile, a comparison was made for the values of the radius of curvature and the opening angle of the tools, before and after bending the metal sheets. The measurements are made using 3 location marks to determine the position considered along the length of each die. The experimental results obtained can be observed in Figure 8. When evaluating the confidence intervals in each case, it was verified that there is no significantly statistical variation of the values before and after the bending operations. However, for the opening angle, the configuration with  $45^{\circ}$ - $90^{\circ}$ - $45^{\circ}$  printing pattern seem to have a regularization of their geometry, i.e. the confidence intervals seem to be smaller after bending. This phenomenon could be a confirmation of a greater compaction of the layers (respect to the other orientations), which allows to increase the rigidity of the part and make the deformation of the tool more stable during the bending process.

Meanwhile, the die insert with a print pattern  $45^{\circ}$ - $0^{\circ}$ - $45^{\circ}$  exhibits some enlargement of its corner radii. All other printing pattern have roughly the same performance, with virtually no modifications after bending. This change on the radius of curvature partly explains the instability observed with this die, for the bend angle of the last set of 20 aluminium sheets.

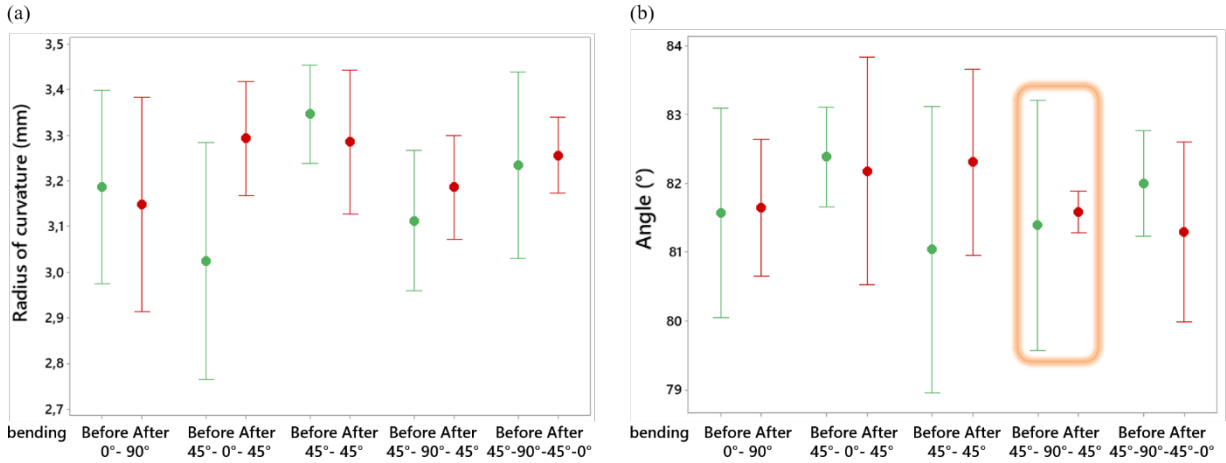


Figure 8.(a) Interval plot for the radius of curvature with PLA dies, (b) interval plot for the opening angle with PLA dies.

For a further analysis of the dimensional changes occurred in the die after bending, possible changes in the roughness of the edges were also measured. The surface roughness is measured considering the two mean arithmetic roughness Ra and waviness Wa parameters. The roughness is mainly related to the changes produced in a local region, which can occur both by the manufacturing process itself (because of wear and/or compression) and by other factors such as the structure of the material. Meanwhile, the waviness considers measurements in the irregularities of the surface, of greater length than the roughness of the surface, which are caused mainly by the layer-wise and discrete additive nature of the 3D printing process. The test is performed using a probe that travels 5 mm on the surface of two different areas of the die (the corners). The results are shown in Figure 9.

In general, for all the printing patterns, the waviness measurements do not show differences for the values obtained before and after bending. However, some little variations in surface roughness can be found, mostly in the dies with a large after bending. For both cases, the mean roughness value is higher. In general, the rise in surface roughness in the case of bending tools may be due to transport and removal of material on the surface of the areas of high stress concentration, due to friction between the PLA and the metal sheets during the bending process. The results for these two configurations are very interesting: while their geometrical surface profile is more stable and the obtained bending angle is also more stable with these two dies, their surface deteriorates at a microscopic level. This means that these two configurations compress and deform less than the others, hence they experience a larger level of stress and a larger level of frictional stress, which leads to die wear. On the contrary, the high concentration of loads on the die corners may produce the opposite effect on other configurations. In fact, it was observed that with a print pattern of 0°-90° or 45°-0°-45°, the confidence intervals of the bend angle increase over time. This means that these die inserts react by deforming themselves during the bending process, thus reducing the contact stresses and the consequent wear. The forming load tends to crush the waviness peaks on the surface of the die. As seen in Figure 9, there is tendency for Wa to be reduced after bending for the 0°-90° and the 45°-0°-45°.

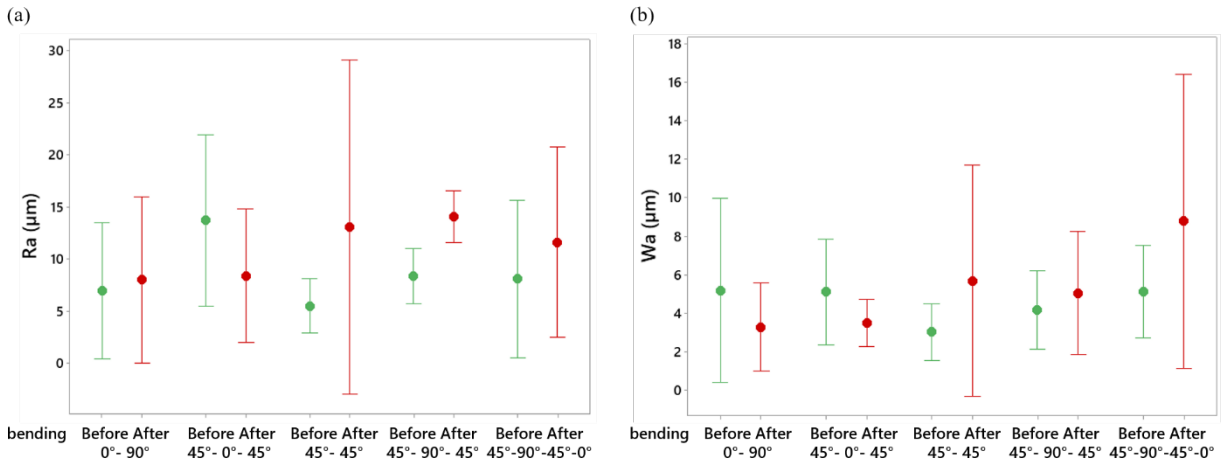


Figure 9.(a) Interval plot of surface roughness, (b) interval plot of waviness.

A careful observation and a comparison of figures 8 and 9 gives an interesting insight into the behaviour of these 3D printed rapid tools. The wear is limited (no significant weight change has been observed with a precision scale). However, the modification of roughness clearly indicates that some kind of surface modification has occurred. There seem to be a negative correlation between the compression of the corner radii (measured through the average change of the curvature radius before and after bending tests and surface modification) and the modification of surface (measured through the average change of roughness  $Ra$  before and after the tests). In other words, 3D printed configurations that tend to collapse under the forming load suffer a lower surface wear, and viceversa. This correlation is very clear and reported in Figure 10, which shows a nearly specular shape of the two scatterplots of corner radius and roughness change vs. the change of standard deviation of the bending angle before and after the bending tests cycle. The die inserts with the  $45^\circ-45^\circ$  and the  $45^\circ-90^\circ-45^\circ$  patterns exhibit a negligible corner radius change, with an improvement of the angle standard deviation, at the expense of a large variation of surface roughness.

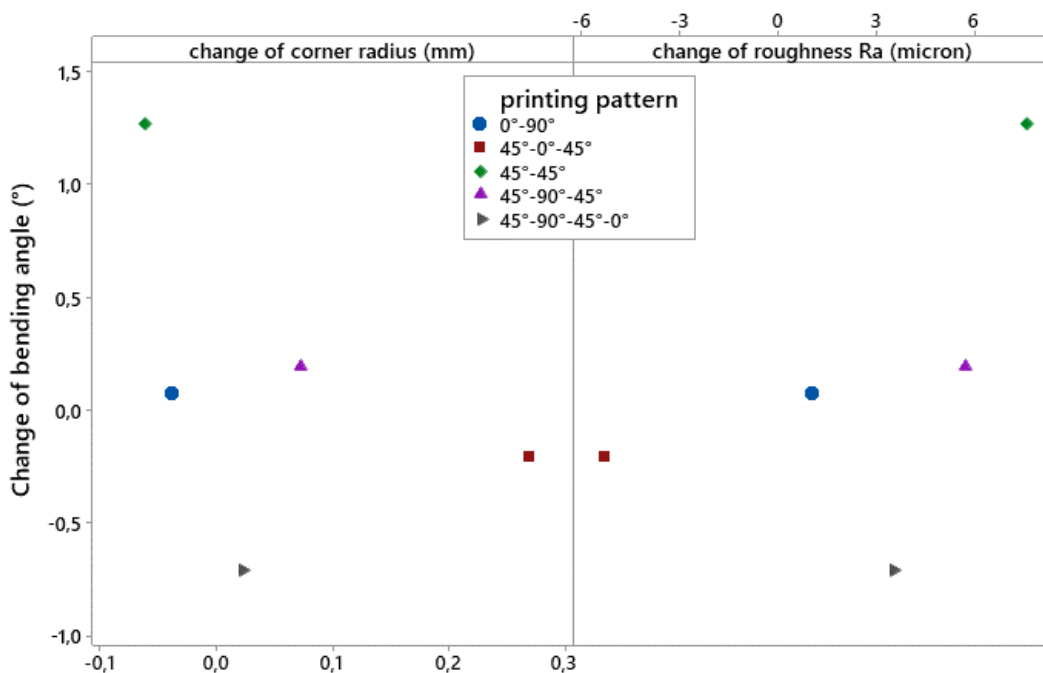


Figure 10. average values of change of corner radius and surface roughness before and after the bending tests, plotted vs. the change of standard deviation of bending angle.

## 4. Conclusions

The use of polymeric tools, 3D printed by FDM, in the sheet metal air bending process is stable over time for small production batches. The results obtained show that with a suitable combination of materials and printing parameters, it is possible to 3D print polymeric inserts with high mechanical resistance, that allow good performance during air bending. A study was made considering two different types of polymeric tools.

A first study was carried out using a printed polycarbonate (PC) insert for the bending of two types of steel sheets:

- The compression tests on 3D printed PC samples showed that using a larger tool tip (T16 instead of T12) increases the compressive stiffness (i.e. the elastic modulus  $E$ ) and the yield stress.
- FEM simulations have shown that the critical regions are the die corners and that, with the tested die geometry, a mild steel can be bent with a maximum thickness of 1.5 mm.
- The experimental bending tests showed that the use of 3D printed polycarbonate die inserts is feasible for small batches, for thin sheets (1.5 mm) of mild and stainless steel. The tests show that the final bend angle after springback stabilises after the 30<sup>th</sup> bend cycle (and finally starts increasing again after the 130<sup>th</sup> test).

In a second, deeper study, PLA inserts were used for the bending of aluminium and steel sheets, to study the effect of the printing parameters on the mechanical properties of the tools.

It was observed that by modifying the printing pattern it is possible to induce minor differences in the properties and the behaviour of the rapid die inserts.

- The compression tests on 3D printed PLA samples showed that a 0°-90° printing pattern decreases the mechanical properties, while the best and most repeatable compression results are obtained with the “standard” 45°-45° and the 45°-0°-45°-90° patterns.
- Overall, the observed variations (after 60 bending tests) of bend angles (fig. 7), geometry of die inserts (fig. 8) and surface roughness (fig. 9) are very limited for all dies, and this show that 3D printed PLA inserts can effectively be used for short run bending operations.
- However, minor variations of angle do occur, and little differences can be appreciated among the different printing patterns. The repeated bending tests show that v-dies 3D printed with a 45°-45°, 45°-90°-45° or 45°-0°-45°-90° stabilize the angle deviation during the bending process. Surprisingly, the most stable behaviour is not observed with the standard 45°-45° pattern, but with the alternated 45°-90°-45° pattern, for which the angle deviation never exceeds  $\pm 0.5^\circ$ . On the contrary, die inserts with a printing pattern equal to 0°-90° and 45°-0°-45° have a more unstable performance over time.
- Comparing the results of figures 7 (variation), 8 (variation of), 9 (variation of of dies) and 10, the best compromise and the most stable behaviour can be attributed to the 45°-90°-45° print pattern. This pattern offered higher repeatability in the measurements during the whole bending process for the bend angle.

## Acknowledgments

The authors wish to acknowledge and thank the cooperation of the Italian company Rolleri SpA, a producer of press brake tools, which provided the press, the dies and the sheet materials for the preliminary study on polycarbonate inserts.

The authors declare that they have no conflict of interest.

## References

- [1] de Souza JHC, Liewald M. Analysis of the tribological behaviour of polymer composite tool materials for sheet metal forming. *Wear* 2010;268:241–8. <https://doi.org/10.1016/j.wear.2009.07.017>.
- [2] Naghshineh B, Carvalho H. The Impact of Additive Manufacturing on Supply Chain Resilience. In: Camarinha-Matos LM, Farhadi N, Lopes F, Pereira H, editors. *Technol. Innov. Life Improv.*, Cham: Springer International Publishing; 2020, p. 214–21.



- [3] Sachs E, Cima M, Cornie J. Three-Dimensional Printing: Rapid Tooling and Prototypes Directly from a CAD Model. *CIRP Ann* 1990;39:201–4. [https://doi.org/10.1016/S0007-8506\(07\)61035-X](https://doi.org/10.1016/S0007-8506(07)61035-X).
- [4] Park Y, Colton JS. Failure Analysis of Rapid Prototyped Tooling in Sheet Metal Forming—V-Die Bending. *J Manuf Sci Eng* 2005;127:116. <https://doi.org/10.1115/1.1828053>.
- [5] Zaragoza VG, Strano M, Iorio L, Monno M. Sheet metal bending with flexible tools. *Procedia Manuf.*, vol. 29, Elsevier; 2019, p. 232–9. <https://doi.org/10.1016/j.promfg.2019.02.131>.
- [6] Pinto M, Santos AD, Teixeira P, Bolt PJ. Study on the usability and robustness of polymer and wood materials for tooling in sheet metal forming. *J Mater Process Technol* 2008;202:47–53. <https://doi.org/10.1016/j.jmatprotec.2007.08.082>.
- [7] Xu J, Zhang J, Cui J, Zhang X. Characteristics of drawing process of AA5182 aluminum alloy sheet during rubber-pad forming. *Int J Adv Manuf Technol* 2018;96:1139–48. <https://doi.org/10.1007/s00170-018-1616-7>.
- [8] Lee J, Park H, Kim SJ, Kwon YN, Kim D. Numerical investigation into plastic deformation and failure in aluminum alloy sheet rubber-diaphragm forming. *Int J Mech Sci* 2018;142–143:112–20. <https://doi.org/10.1016/j.ijmecsci.2018.04.022>.
- [9] Iorio L, Pagani L, Strano M, Monno M. Design of Deformable Tools for Sheet Metal Forming. *J Manuf Sci Eng* 2016;138:094701. <https://doi.org/10.1115/1.4034006>.
- [10] Witulski J, Trompeter M, Tekkaya AEE, Kleiner M. High wear resistant deep drawing tools made of coated polymers. *CIRP Ann - Manuf Technol* 2011;60:311–4. <https://doi.org/10.1016/j.cirp.2011.03.149>.
- [11] Leal R, Barreiros FM, Alves L, Romeiro F, Vasco JC, Santos M, et al. Additive manufacturing tooling for the automotive industry. *Int J Adv Manuf Technol* 2017;92:1671–6. <https://doi.org/10.1007/s00170-017-0239-8>.
- [12] Masood SH. Intelligent rapid prototyping with fused deposition modelling. *Rapid Prototyp J* 1996;2:24–33. <https://doi.org/10.1108/13552549610109054>.
- [13] Nakamura N, Mori K ichiro, Abe F, Abe Y. Bending of sheet metals using plastic tools made with 3D printer. *Procedia Manuf* 2018;15:737–42. <https://doi.org/10.1016/j.promfg.2018.07.312>.
- [14] Smith WC, Dean RW. Structural characteristics of fused deposition modeling polycarbonate material. *Polym Test* 2013;32:1306–12. <https://doi.org/10.1016/j.polymertesting.2013.07.014>.
- [15] Hernandez R, Slaughter D, Whaley D, Tate J, Asiabanpour B. Analyzing the Tensile, Compressive, and Flexural Properties of 3D Printed ABS P430 Plastic Based on Printing Orientation Using Fused Deposition Modeling. *Proc 27th Annu Int Solid Free Fabr Symp* 2016:939–50.
- [16] Sood AK, Ohdar RK, Mahapatra SS. Parametric appraisal of mechanical property of fused deposition modelling processed parts. *Mater Des* 2010;31:287–95. <https://doi.org/10.1016/j.matdes.2009.06.016>.
- [17] Belter JT, Dollar AM. Strengthening of 3D printed fused deposition manufactured parts using the fill compositing technique. *PLoS One* 2015;10:1–19. <https://doi.org/10.1371/journal.pone.0122915>.
- [18] Mazzanti V, Malagutti L, Mollica F. FDM 3D printing of polymers containing natural fillers: A review of their mechanical properties. *Polymers (Basel)* 2019;11. <https://doi.org/10.3390/polym11071094>.
- [19] ASTM D695. ASTM D695 – 15: Standard Test Method for Compressive Properties of Rigid Plastics 1 Standard Test Method for Compressive Properties of Rigid Plastics. *Am Soc Test Mater* 2015:19428–2959. <https://doi.org/10.1520/D0695-15>.
- [20] Schuh G, Bergweiler G, Bickendorf P, Fiedler F, Colag C. Sheet Metal Forming Using Additively Manufactured Polymer Tools. *Procedia CIRP* 2020;93:20–5. <https://doi.org/10.1016/j.procir.2020.04.013>.
- [21] Anderson EH. The Effect of Porosity on Mechanical Properties of Fused Deposition Manufactured Polymers and Composites 2019.
- [22] Al-Maharma AY, Patil SP, Markert B. Effects of porosity on the mechanical properties of additively manufactured components: a critical review. *Mater Res Express* 2020;7. <https://doi.org/10.1088/2053-1591/abcc5d>.
- [23] Keleş Ö, Anderson EH, Huynh J. Mechanical reliability of short carbon fiber reinforced ABS produced via vibration assisted fused deposition modeling. *Rapid Prototyp J* 2018;24:1572–8. <https://doi.org/10.1108/RPJ-12-2017-0247>.
- [24] Nakamura N, Mori K ichiro, Abe Y. Applicability of plastic tools additively manufactured by fused deposition modelling for sheet metal forming. *Int J Adv Manuf Technol* 2020;108:975–85. <https://doi.org/10.1007/s00170-019-04590-5>.